Research Article

Therapeutic effects of dental pulp stem cells on vascular dementia in rat models

https://doi.org/10.4103/1673-5374.303042

Date of submission: June 3, 2020

Date of decision: July 27, 2020

Date of acceptance: November 3, 2020

Date of web publication: January 7, 2021

Xue-Mei Zhang[#], Yang Sun[#], Ying-Lian Zhou, Zhuo-Min Jiao, Dan Yang, Yuan-Jiao Ouyang, Mei-Yu Yu, Jin-Yue Li, Wei Li, Duo Wang, Hui Yue, Jin Fu[*]

Graphical Abstract *Dental pulp stem cell (DPSC) transplantation is effective for treating vascular dementia*

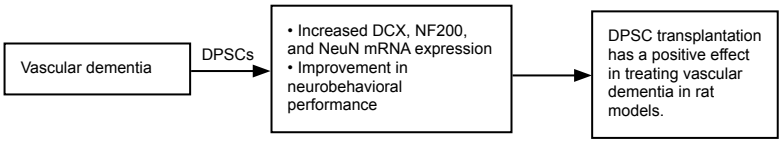

Abstract

Dental pulp stem cells are a type of adult stem cells with strong proliferative ability and multi-differentiation potential. There are no studies on treatment of vascular dementia with dental pulp stem cells. In the present study, rat models of vascular dementia were established by two-vessel occlusion, and 30 days later, rats were injected with 2×10^7 dental pulp stem cells via the tail vein. At 70 days after vascular dementia induction, dental pulp stem cells had migrated to the brain tissue of rat vascular dementia models and differentiated into neuron-like cells. At the same time, doublecortin, neurofilament 200, and NeuN mRNA and protein expression levels in the brain tissue were increased, and glial fibrillary acidic protein mRNA and protein expression levels were decreased. Behavioral testing also revealed that dental pulp stem cell transplantation improved the cognitive function of rat vascular dementia models. These findings suggest that dental pulp stem cell transplantation is effective in treating vascular dementia possibly through a paracrine mechanism. The study was approved by the Animal Ethics Committee of Harbin Medical University (approval No. KY2017-132) in 2017.

Key Words: animal model; dental pulp stem cells; paracrine; repair; stem cells; transplantation; vascular dementia

Chinese Library Classification No. R456; R741; Q983+.8

Introduction

With the progression of society and medical treatment, aging of the population is becoming increasingly evident. The prevalence of dementia has also increased. Vascular dementia (VaD) is the most common cause of dementia, immediately followed by Alzheimer's disease (Rockwood et al., 2000; Jin and Liu, 2019; Zhu et al., 2020). The prevalence of moderate or severe dementia in people aged 65 years and older is approximately 5% (Williams et al., 2000). Dementia patients experience cognitive deficits, dysmnesia, depression, anxiety, and a decline in daily living capacity, all of which increase family and social economic burdens.

Many causes of VaD exist, including hypoperfusion, cerebral small vessel disease, critical infarct, hemorrhage/microbleeding, and hereditary vasculopathy. Hypoperfusion is considered the leading cause of VaD (Venkat et al., 2015), and the rat model of two-vessel occlusion (2-VO) (Nanri and Watanabe, 1999) is a widely used model of cerebral hypoperfusion that has been used to study VaD for many years. We chose Sprague-Dawley rats as experimental animals because, similar to humans, they have a complete circle of Willis (Nanri and Watanabe, 1999). The most commonly used 2-VO rat model mainly exhibits damage of the white matter, leading to neuronal necrosis and damage to neurons in the cerebral cortex and hippocampus (Soria et al., 2013).

Few drugs and no surgical treatments are available for VaD, and no effective drug treatments have been identified. Prevention of this disease, including controlling high-risk factors, such as hypertension, diabetes, hyperlipidemia, smoking, and drinking, is particularly important. Because of the co-existing Alzheimer's disease-related neuropathology, conventional therapeutic drugs for VaD include memantine, galantamine, donepezil, rivastigmine, huperzine, and most drugs associated with acetylcholinesterase inhibition (Baskys and Cheng, 2012). In China, some traditional Chinese medicines and acupuncture are used to treat VaD (Suh et al., 2008). However, the effects of these treatments are not ideal.

Clinical and experimental trials have shown that stem cell transplantation is a potential therapy for multiple diseases, such as those involving the blood, nervous system (Zhang et al., 2010; He et al., 2017; Liu et al., 2019), digestive system (Cao et al., 2017), and circulatory system (Gandia et al., 2008). Bone marrow mesenchymal stem cells have been widely used for the treatment of nervous system diseases (Zhang et al., 2010, 2011). Dental pulp stem cells (DPSCs) derived from pulp tissue, which were first extracted through enzyme digestion by Gronthos et al. (2000), are of mesenchymal origin and,

Department of Neurology, The 2nd Affiliated Hospital of Harbin Medical University, Harbin, Heilongjiang Province, China

*Correspondence to: Jin Fu, PhD, MD, fujin@hrbmu.edu.cn.

https://orcid.org/0000-0001-7532-784X (Jin Fu)

#Both authors contributed equally to this work.

Funding: *This study was supported by Yu Weihan Fund for Distinguished Young Scholars of Harbin Medical University of China, No. 002000013 (to XMZ).*

How to cite this article: *Zhang XM, Sun Y, Zhou YL, Jiao ZM, Yang D, Ouyang YJ, Yu MY, Li JY, Li W, Wang D, Yue H, Fu J (2021) Therapeutic effects of dental pulp stem cells on vascular dementia in rat models. Neural Regen Res 16(8):1645-1651.*

in some circumstances, have strong proliferative ability and multi-differentiation potential. They also have the advantages of simple extraction, easy amplification, and convenient storage (Woods et al., 2009). Therefore, in this study, we chose to inject DPSCs into a 2-VO model to determine whether DPSCs may be an effective treatment for VaD.

Methods and Materials

Study design

A total of 250 male Sprague-Dawley rats were randomly divided into control, sham, VaD, VaD + phosphate buffered saline (PBS), and VaD + DPSCs groups (n = 50/group). The control group did not receive any treatment, and the sham group underwent a sham operation. The VaD, VaD + PBS, and VaD + DPSCs groups underwent surgery to induce 2-VO.

All animals were habituated to the eight-arm maze training environment on days 34–39. On days 40–49, all animals underwent adaptive behavior training in the eight-arm maze. On day 50, DPSCs were injected into the tail veins of the rats. On days 60–69, all animals underwent eight-arm maze behavioral testing. On day 70, tissues from all animals were harvested for subsequent experiments. The general experimental procedure is shown in **Figure 1A**.

Animal selection and 2-VO model establishment

In total, 150 male Sprague-Dawley rats weighing 200–220 g were used to establish the 2-VO model, and 40 male Sprague-Dawley rats weighing approximately 40 g were selected as DPSC donor animals. The rats were purchased from the Animal Experiment Center of the Second Affiliated Hospital of Harbin Medical University (license No. SCXK (Hei) 2013-001). All procedures and euthanasia were performed in accordance with the Guidelines of the Animal Ethics Committee of Harbin Medical University, and the study was approved by the Animal Ethics Committee of Harbin Medical University (approval No. KY2017-132) in 2017. The animals were housed in the Animal Experiment Center of the Second Affiliated Hospital of Harbin Medical University under a controlled temperature and a 12-hour light/dark cycle. All animals were appropriately anesthetized during the operation. Food and water were withheld before the operation.

The animals were anesthetized by intraperitoneal injection of pentobarbital sodium (40 mg/kg; X-Y Biotechnology, Shanghai, China). Once the rats ceased responses to pain stimulation and exhibited no corneal reflex, they were immobilized and placed in the prone position. Under anesthesia, the skin of the neck was disinfected, a 1.5-cm incision was made along the neck, and the muscles were bluntly dissected. The carotid sheath was sufficiently exposed, and carotid pulsation was observed. The carotid artery and nerve were then separated. The bilateral common carotid artery was ligated with a surgical suture, and then the muscle and skin were sutured (**Figure 1B**). The rats were kept warm and provided a normal diet after regaining consciousness (Venkat et al., 2015).

DPSC culture

The rats were placed in 75% ethyl alcohol after cervical amputation. The incisors were acquired in an aseptic manner. The tissue around the teeth was removed, and the cells were placed in petri dishes containing sterile PBS. Then, the cells were transported to the cell culture room. The tissue was removed again, and the teeth were cut open with a small pair of scissors. The pulp was extracted with a pulp needle, and the pulp tissue was sheared in PBS with microscissors. The mixed suspension was collected in a centrifuge tube for centrifugation at 168 × g for 5 minutes. The supernatant was discarded, and then the suspension was precipitated with 0.3% collagenase I (Sigma-Aldrich, Shanghai, China) and centrifuged again after shaking for 40 minutes in the dark. The supernatant was discarded, and complete culture medium (20% fetal bovine serum (Boster, Wuhan, China), 1% penicillin-streptomycin solution (Solarbio, Beijing, China), and 79% Dulbecco's modified Eagle medium (Solarbio)) was used to resuspend the precipitate. The mixed suspension was placed in a culture flask, which was placed in an incubator (37°C, 5% CO_2, humidified atmosphere) (Zhang et al., 2010).

Approximately 1 week later, the suspension was turbid, and partial cell adhesion was observed. The complete culture medium was exchanged, after which the cells began growing rapidly. The medium was replaced every 3 days, and when the cells reached 80% confluence, they were digested with trypsin and passaged at a ratio of 1:2. The cells were passaged three times.

Identification of DPSCs by flow cytometry

We used third-generation DPSCs for flow cytometry. The cells were washed with PBS after trypsin (Solarbio) digestion. Fluorescein isothiocyanate-conjugated anti-rat CD29 (1:200; Cat# 561796; BD Biosciences, Shanghai, China), allophycocyanin-conjugated anti-rat CD90 (1:200; Cat# 561409; BD Biosciences), phycoerythrin-conjugated anti-rat CD34 (1:200; Cat# ab213058; Abcam, Shanghai, China), and phycoerythrin-conjugated anti-rat CD45 (1:200; Cat# 554878; BD Biosciences) fluorescent antibodies were used. Cells were incubated with the fluorescent antibodies for 1 hour and then placed in a flow cytometer (Beckman Coulter, Shanghai, China) for testing.

In vitro induction of DPSCs

According to the instructions of the rat bone marrow mesenchymal stem cell adipogenic induction culture medium A and B (Cat# RASMX-90031; Cyagen, Suzhou, China), third-generation DPSCs were digested with trypsin and cultured in six-well plates (2×10^4 cells/cm^2). An appropriate amount of complete culture medium (20% fetal bovine serum, 1% penicillin-streptomycin solution, and 79% Dulbecco's modified Eagle medium) was added, and the cells were cultured to 100% or greater confluence, after which the medium was exchanged with medium A (rat bone marrow mesenchymal stem cell adipogenic differentiation fetal bovine serum, penicillin-streptomycin, glutamine, insulin, 3-isobutyl-1-methylanxthine, rosiglitazone, and dexamethasone). After 3 days, the medium was exchanged with medium B (rat bone marrow mesenchymal stem cell adipogenic differentiation fetal bovine serum, penicillin-streptomycin, glutamine, and insulin). After 24 hours, the medium was exchanged with medium B again. This cycle of induction was repeated several times (three or five cycles) until large, round lipid droplets were observed. After the cells had differentiated, the induction medium was removed. The cells were fixed with 4% formaldehyde for 20 minutes after being rinsed three times with PBS. Then, the cells were rinsed with PBS, and oil red O staining solution (Cyagen) was added for 30 minutes (Shi et al., 2019).

According to the instructions of the rat bone marrow mesenchymal stem cell osteogenic induction culture medium (Cat# RASMX-90021; Cyagen), third-generation DPSCs were digested with trypsin and cultured in six-well plates precoated with 0.1% gelatin solution (2×10^4 cells/cm^2). An appropriate amount of complete medium was added, and the cells were cultured to 60–70% confluence; after this, the medium was exchanged with induction culture medium (rat bone marrow mesenchymal stem cell osteogenic differentiation fetal bovine serum, penicillin-streptomycin, glutamine, ascorbate, β-glycerophosphate, and dexamethasone). The medium was exchanged every 3 days, and after 2–4 weeks, changes in cell morphology and growth were observed under a microscope. After the cells had differentiated, the induction medium was removed. The cells were fixed with 4% formaldehyde solution for 20 minutes after being rinsed three times with PBS. Then, the cells were rinsed with PBS, and Alizarin red staining

solution (Cyagen) was added for 3–5 minutes (Luo et al., 2019).

In vivo induction and transplantation of DPSCs

Third-generation DPSCs (2×10^7 cells) were washed in a flask with Dulbecco's modified Eagle medium after being digested with trypsin. The cells were centrifuged, and the liquid supernatant was removed so that the volume was less than 25 μL. The cells were kept in the dark to avoid quenching of the dye. A total of 1 mL of diluent C was added to the cells (2×10^7 cells), and 4 μL of PKH67 staining solution (Cat# PKH67GL MSDS; Sigma-Aldrich) was added to 1 mL of diluent C. The solutions were mixed immediately and periodically throughout incubation at 37°C for 5 minutes. An equivalent amount of serum was added to terminate the reaction. The cells were centrifuged at 1000 r/minute for 5 minutes and then suspended in complete culture medium and centrifuged three times. Some suspensions were dropped onto glass slides to observe PKH67 staining. On day 50, 1 mL of PBS containing 2×10^7 DPSCs was injected into the tail veins of rats.

Histopathological examination

On day 70, the animals were euthanized with an overdose of anesthesia administered in the abdominal cavity. The animals were transcardially perfused with PBS followed by 4% paraformaldehyde for 20 minutes each. Brain tissues were removed and soaked in 4% paraformaldehyde for 3 days. The tissues were embedded in paraffin blocks and then cut into slices. The sections were kept in a wet box at 4°C in the dark. The slides were then washed with PBS in a darkroom, and goat serum was applied to the slides for 30 minutes. The goat serum was removed, and the sections were incubated with rabbit anti-rat glial fibrillary acidic protein (GFAP; 1:100; Cat# ab33922; Abcam), mouse anti-rat doublecortin (DCX; 1:100; Cat# ab18723; Abcam), mouse anti-rat neuronal nuclear protein (NeuN; 1:100; Cat# ab177487-100; Abcam), and mouse anti-rat neurofilament 200 (NF200; 1:80; Cat# ab82259; Abcam) antibodies at 4°C overnight in a wet box. The cells were washed again with PBS and then incubated with tetramethylrhodamine-conjugated AffiniPure goat anti-mouse IgG (1:50; Cat# ZF-0313; ZSGB, Beijing, China) or tetramethylrhodamine-conjugated AffiniPure goat anti-rabbit IgG (1:50; Cat# ZF-0316; ZSGB) at 37°C for 30 minutes. The nuclei were stained with 4',6-diamidino-2-phenylindole (Cat# C1005; Beyotime, Shanghai, China) for 10 minutes. The cells were washed with PBS again, and antifade mounting medium (Cat# p0126; Beyotime) was added to prevent quenching. After the cerebral cortex slices were dewaxed and hydrated, they were stained with hematoxylin for 5 minutes. They were then washed with a stream of water for 5 minutes and immersed in 1% hydrochloric alcohol for 5 minutes. After washing, the slices were stained with eosin for 3 minutes and sealed with neutral resin after another wash and dehydration. The results were observed with a confocal laser scanning microscope (Olympus, Tokyo, Japan).

Real-time polymerase chain reaction

Total RNA was harvested from cerebral cortex samples using the TRIzol reagent (Cat# R0016; Beyotime). The RNA concentration of the samples was determined by ultraviolet spectrophotometry (NANO 2000; Thermo Fisher Scientific, Waltham, MA, USA). The obtained RNA samples were reverse transcribed to obtain the corresponding cDNA. Real-time fluorescence quantitative analysis (exicycler96; Bioneer Corporation, Daejeon, Korea) was performed. The target gene primers were as follows: GFAP: forward: 5′-CAA GAG GAA CAT CGT GGT AAA GAC-3′, reverse: 5′-CGA GCC GTG GGC ATA AAA-3′; DCX: forward: 5′-TCC TCA TAG CCA CGC TCC C-3′, reverse: 5′-CGT ACA GAT CAC GTT GCC CTA A-3′, Rbfox3 (NeuN): forward: 5′-CAC CGC CGT CGC CTA TC-3′, reverse: 5′-CCA GTG CCG CTC CGT AAG-3′, Nefh (NF200): forward: 5′-GGA GGA CCG TCA TCA GGT AGA C-3′, reverse: 5′-TTT CTG TAA GCA GCG ATC TCA AT-3′.

Western blot analysis

On day 70, samples from the cerebral cortex were collected on ice and stored at –80°C in a freezer. The samples were lysed with lysis solution mixed with 1% phenylmethylsulfonyl fluoride to isolate the protein, and the protein concentration of each sample was determined. The electrophoresis device was assembled, and the proteins were subjected to sodium dodecyl sulfate polyacrylamide gel electrophoresis and then transferred to a polyvinylidene fluoride membrane (Cat# FFP24; Beyotime). After the membrane was blocked with 1% bovine serum albumin (Cat# ST023-50g; Beyotime), it was incubated overnight with the following primary antibodies: rabbit anti-rat GFAP (1:500), mouse anti-rat DCX (1:500), mouse anti-rat NeuN (1:1000), and mouse anti-rat NF200 (1:200). After washing with Tris-buffered saline with Tween-20, the corresponding secondary antibodies (horseradish peroxidase-conjugated goat anti-rabbit IgG (1:5000; Cat# WLA023; Wanleibio, Shenyang, China) and horseradish peroxidase-conjugated rabbit anti-mouse IgG (1:5000; Cat# WLA024; Wanleibio)) were added and incubated for 45 minutes at 37°C. The electrochemiluminescence reagent (Cat# P0018S; Beyotime) was added and exposed in the darkroom. The data were analyzed with Gel-Pro-Analyzer (Cat# 9413B; Beijingliuyi, Beijing, China).

Behavioral test

The eight-arm maze was used to perform behavioral testing (Kurzina et al., 2020). On days 34–39 after modeling, the animals were placed into the maze for habituation. The behavioral test was divided into two parts: sessions performed during days 40–49 and sessions performed during days 60–69. Food intake was restricted in all animals. Behavioral data were mainly collected on days 68 and 69. On day 40, the door leading to each arm was opened, and the animals were allowed to freely move through the central circular area for 10 minutes. The same procedure was repeated on days 41–43. This process was used to familiarize the animals with the maze environment and habituate them to the behavioral test. From the 44th day, the animals were trained individually. Food (food granules approximately 3 mm in diameter) was placed in four randomly selected arms; one piece of food was placed in each arm, and the animal was allowed to feed freely. The animal was removed after all of the food was eaten or after 10 minutes. The procedure was repeated on days 45–47. On days 48–49, the door was closed, an animal was placed in the central circular area for 30 seconds, and then the door was opened to allow the animal to search for food in the maze until it had eaten all of the food in the immobilized arm. On days 50–59, the procedure performed on days 40–49 was repeated with food in the same arm of the maze as previously presented. If uneaten food remained after 10 minutes, the latency was recorded as 10 minutes. We also recorded the number of times the rats erroneously entered the incorrect arm, and if more than 15 entries into the incorrect arm occurred, the score was recorded as 15.

Statistical analysis

All of the data were processed by SPSS 23.0 statistical analysis software (IBM, Armonk, NY, USA), and quantitative data are expressed as the mean ± standard deviation (SD). When the data showed homogeneity of variance, differences among groups were analyzed by one-way analysis of variance, and *t*-tests were used for comparisons between two groups. The difference was considered statistically significant if $P < 0.05$.

Results

Successful VaD modeling

Compared with the sham group, the VaD group exhibited

obviously constricted cells, a widened vascular space, and inflammatory cell infiltration after the 2-VO operation (**Figure 1C**). Comparison of the changes in the cells between the groups indicated that the model was successfully established.

Identification of DPSCs

To verify that the cells extracted were DPSCs, we induced cell differentiation and performed flow cytometry analysis. Primary DPSCs began to adhere to the wall after approximately 7 days, at which point the cells were fusiform in shape with fibers and protrusions. After approximately 14 days, cell confluence reached 80–90%. After passage, the cells grew rapidly and filled the culture flask after approximately 3 days. Third-generation DPSCs, which were used for transplantation, were induced to undergo osteogenesis and adipocyte differentiation. As shown in **Figure 2A**, third-generation DPSCs exhibited a fusiform fiber-like morphology. After induction, DPSCs differentiated into adipocytes and formed lipid droplets detected by oil red O staining (**Figure 2B**) and calcium deposits under Alizarin red staining (**Figure 2C**). Flow cytometry showed high CD29 and CD90 expression and low CD34 and CD45 expression on the cell surface (**Figure 2E–H**). All of the above results indicated that the extracted cells were DPSCs.

Migration and differentiation of DPSCs *in vivo*

After the cells were stained with PKH67 dye, they fluoresced green when excited at 488 nm under a fluorescence microscope (**Figure 2D**). The results showed that fluorescent labeling of the cell surface was successful. After injection of the fluorescently labeled cells, the immunofluorescence results showed that green fluorescence was found in the brain tissue, indicating that the transplanted DPSCs had migrated into the brain (**Figure 3**).

DPSCs increase the number of DCX, NF200, and NeuN positive cells in the cerebral cortex of VaD rats

The immunohistochemical staining results showed that compared with the control group, the percentage of DCX, NF200, and NeuN positive cells in the cerebral cortex was lower ($P < 0.05$) and the percentage of GFAP positive cells was higher ($P < 0.05$) in rats in the VaD group. Therefore, after the modeling process, DCX, NF200, and NeuN expression decreased, and GFAP expression increased. The percentage of DCX, NF200, and NeuN positive cells in the cerebral cortex in the VaD + DPSCs group was higher than that in the VaD + PBS group, ($P < 0.05$), and the percentage of GFAP positive cells was lower than that in the VaD + PBS group ($P < 0.05$; **Figure 4**).

DPSCs increase DCX, NF200, and NeuN protein expression in the cerebral cortex of VaD rats

The western blot results showed that compared with the control group, the DCX, NF200, and NeuN protein expression in the cerebral cortex was lower ($P < 0.05$) and the protein expression of GFAP was higher in the VaD group ($P < 0.05$). Therefore, after the modeling process, DCX, NF200, and NeuN expression decreased, and GFAP expression increased. The DCX, NF200, and NeuN protein expression in the VaD + DPSCs group was higher than that in the VaD + PBS group ($P < 0.05$), and the GFAP protein expression in the VaD + DPSCs group was lower than that in the VaD + PBS group ($P < 0.05$; **Figure 5A–D**).

DPSCs increase the DCX, NF200, and NeuN mRNA expression in the cerebral cortex of VaD rats

Real-time polymerase chain reaction results showed that the mRNA expression of DCX, NF200, and NeuN in the VaD group was lower than that in the control group ($P < 0.05$), and the GFAP mRNA expression in the VaD group was higher than that in the control group ($P < 0.05$). Therefore, after the modeling processing, DCX, NF200, and NeuN expression decreased, and GFAP expression increased. The DCX, NF200, and NeuN mRNA expression in the VaD + DPSCs group was higher than that in the VaD + PBS group ($P < 0.05$), and the GFAP mRNA expression in the VaD + DPSCs group was lower than that in the VaD + PBS group ($P < 0.05$; **Figure 5E–H**).

DPSCs improve the neurobehavioral performance of VaD rats

The results of the eight-arm maze test showed that, compared with the control group, the number of errors and the latency were increased in the VaD group ($P < 0.05$), indicating that the VaD model was successfully established. The number of errors and the latency in the VaD + DPSCs group were lower than those of the VaD + PBS group ($P < 0.05$; **Figure 6**).

Discussion

VaD is a disease that is influenced by multiple pathophysiological and risk factors, either alone or in combination, and is mainly caused by the reduction of blood flow in the brain. Permanent ligation of the bilateral common carotid arteries, which causes chronic global cerebral ischemia, is used to induce 2-VO in Sprague-Dawley rats (Farkas et al., 2007). Chronic hypoperfusion leads to failure of energy production in neuronal and glial cells, which can also accelerate the production of amyloid proteins (Mawuenyega et al., 2010). The main pathophysiological changes in this model are neuronal infarction in the cerebral cortex and hippocampus (Soria et al., 2013), gliocyte proliferation (Walker and Rosenberg, 2010), white matter sparsity, white matter damage, and blood-brain barrier destruction. Therefore, in our study, we chose to observe samples from the cerebral cortex. Attention should be paid to the performance of model animals in behavior tests that rely on vision. Some models may have visual impairments because of occlusion of the artery that supplies the optic nerve (Yamamoto et al., 2006).

Many experiments have shown that DPSC transplantation is beneficial for the injured nervous system (Mead et al., 2017). Because autologous DPSCs can be used, there is a reduced likelihood of rejection and less ethical controversy. Neural function was improved after DPSC transplantation in a middle cerebral artery occlusion model (Yang et al., 2009). DPSCs injected into the cerebrospinal fluid of rats after cortical injury have been shown to be useful sources of neurons and glia *in vivo* (Király et al., 2011). Transplantation of stem cells from human exfoliated deciduous teeth after traumatic spinal cord injury may have a neuroprotective effect by inhibiting early neuronal apoptosis (Nicola et al., 2017). Additionally, human tooth germ stem cells exert neuroprotective effects in Alzheimer's and Parkinson's disease models by inducing angiogenesis, thus eliciting antioxidative and antiapoptotic effects (Yalvaç et al., 2013). Therefore, in this study, we selected DPSCs as therapeutic agents.

To ensure that the cultured cells were DPSCs, we used culture induction and flow cytometry methods. Because no commercially-available osteogenesis and adipogenic medium exists for DPSCs and because DPSCs are also mesenchymal stem cells, we used bone marrow mesenchymal stem cell osteogenesis and adipogenic medium. Our study confirmed that DPSCs differentiated into osteoblasts and adipocytes after induction and culture. DPSCs express no specific surface markers. Therefore, in this study, two commonly used DPSC markers (CD29 and CD90) and two hematopoietic stem cell markers (CD34 and CD45) were used to identify DPSCs (Huang et al., 2008). The flow cytometry results showed that DPSCs highly expressed CD29 and CD90 and expressed almost no CD34 and CD45. To track transplanted DPSCs and monitor their differentiation in rat brain tissue, we used PKH67, a green cell membrane dye, to label DPSCs before transplantation. Studies have shown that the use of fluorescent dye is an ideal method to label transplanted cells (Nagyova et al., 2014). The results demonstrated that DPSCs migrated to brain tissue and

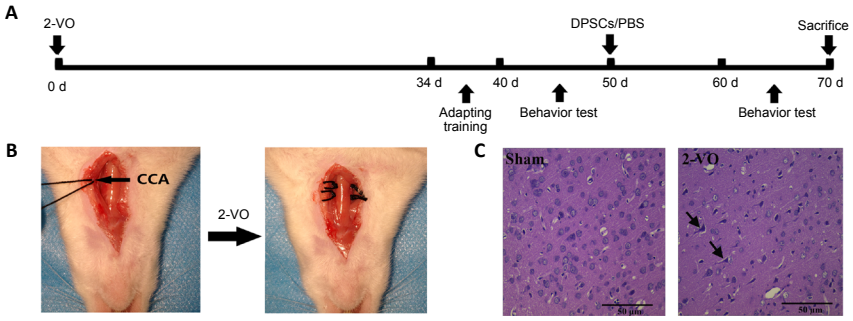

Figure 1 | **Establishment of the 2-VO model.**
(A) Flow chart of the experiment. (B) Ligation process of the CCA. (C) Pathological changes of the cerebral cortex (hematoxylin-eosin staining). The cells in the VaD group were obviously constricted, had a widened vascular space, and exhibited inflammatory cell infiltration. Scale bars: 50 μm. 2-VO: 2-Vessel occlusion; CCA: common carotid artery; DPSCs: dental pulp stem cells; PBS: phosphate buffered saline; VaD: vascular dementia.

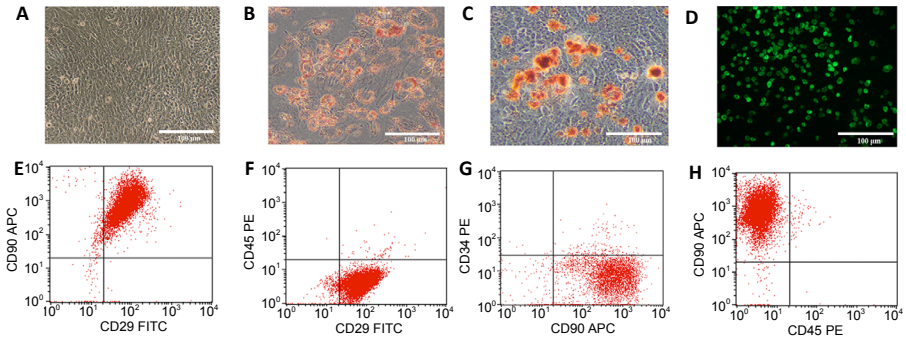

Figure 2 | **Identification of DPSCs.**
(A) Cell morphology of third-generation DPSCs. (B) DPSCs differentiated into adipocytes and formed lipid droplets. (C) Alizarin red staining revealed calcium deposit formation. (D) After staining with PKH67 dye, cells fluoresced green when excited at 488 nm under a fluorescence microscope. Scale bars: 100 μm. (E–H) Identification of DPSCs by flow cytometry; high expression levels of CD29 and CD90 and low expression levels of CD34 and CD45 were found. DPSCs: Dental pulp stem cells.

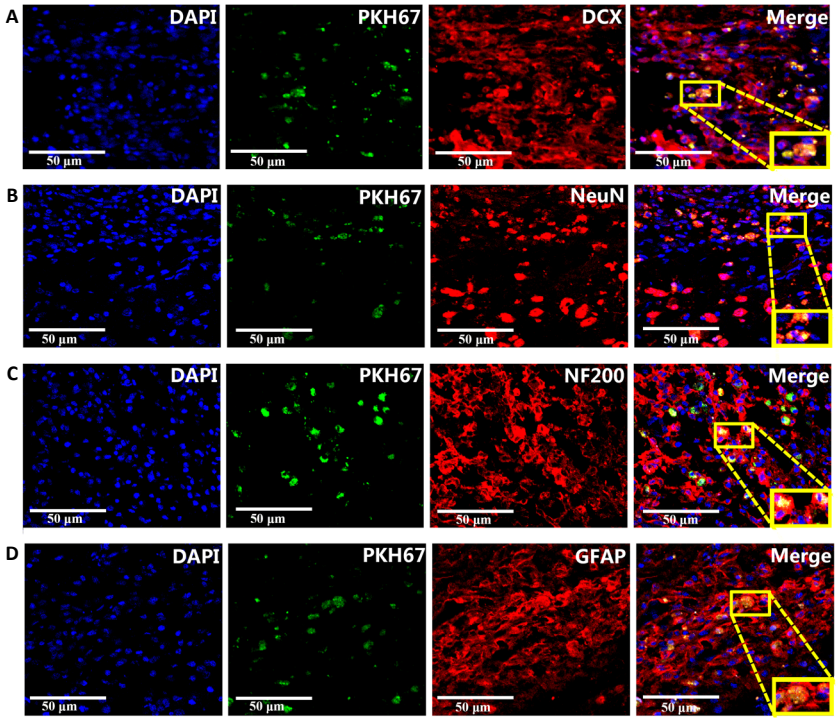

Figure 3 | **Migration and differentiation of DPSCs in the cerebral cortex of vascular dementia rats.**
(A) DCX expression in transplanted DPSCs. (B) NeuN expression in transplanted DPSCs. (C) NF200 expression in transplanted DPSCs. (D) GFAP expression in transplanted DPSCs. Nuclear chromatin was stained with DAPI. The membranes of PKH67-labeled DPSCs fluoresced green. The neuronal marker proteins DCX, NeuN, NF200, and GFAP were stained by tetramethylrhodamine (red). Scale bars: 50 μm. DAPI: 4′,6-Diamidino-2-phenylindole; DCX: doublecortin; DPSCs: dental pulp stem cells; GFAP: glial fibrillary acidic protein; NeuN: neuronal nuclear protein; NF200: neurofilament 200.

differentiated into neuron-like cells in a model of chronic cerebral ischemic damage.

GFAP, an intermediate filament protein, was first found in astrocytes and is now used as a marker of astrocyte formation (Wilhelmsson et al., 2019). Although astrocytes secrete neurotrophic factors and inhibit inflammation, glial scar formation hinders neuron regeneration (Fawcett and Asher, 1999). NeuN is present in a variety of nerve cells and is a marker of mature neurons. Its presence indicates that cells are at the end stage of differentiation (Mullen et al., 1992). NeuN can be used to evaluate the fate of transplanted DPSCs in the brain. NF200 is a neurofilament protein, a hallmark of axons, and a neural precursor cell marker that primarily maintains the structure and morphology of neurons (Porseva, 2013). DCX is a microtubule-associated protein that plays an important role in cell migration. We found that DPSCs could improve the obvious proliferative activity in the injured area of VaD rats. Our results showed that DPSCs transplanted into the 2-VO model differentiated into neuron-like cells, inhibited glial cell growth, promoted nerve cell proliferation, and improved behavioral test results.

These results suggest that DPSC transplantation has a positive effect in treating the VaD model. This effect could occur because when DPSCs are transplanted into the body, they not only differentiate into cells of the damaged tissue to achieve therapeutic effects but also promote axonal growth through a paracrine mechanism and secrete neurotrophic factors and cytokines.

Author contributions: *Study design: XMZ, JF, YS; experimental implementation: YS, YJO, YLZ, DW, HY; data collection: MYY, JYL; data analysis: ZMJ, DY; literature search: WL; manuscript writing: XMZ, YS, JF. All authors read and approved the final manuscript.*
Conflicts of interest: *The authors declare that they have no conflict of interest.*
Financial support: *This study was supported by Yu Weihan Fund for Distinguished Young Scholars of Harbin Medical University of China, No. 002000013 (to XMZ). The funder had no roles in the study design, conduction of experiment, data collection and analysis, decision to publish, or preparation of the manuscript.*
Institutional review board statement: *The study was approved by the Animal Ethics Committee of Harbin Medical University (approval No. KY2017-132) in 2017.*
Copyright license agreement: *The Copyright License Agreement has been signed by all authors before publication.*
Data sharing statement: *Datasets analyzed during the current study are available from the corresponding author on reasonable request.*
Plagiarism check: *Checked twice by iThenticate.*
Peer review: *Externally peer reviewed.*
Open access statement: *This is an open access*

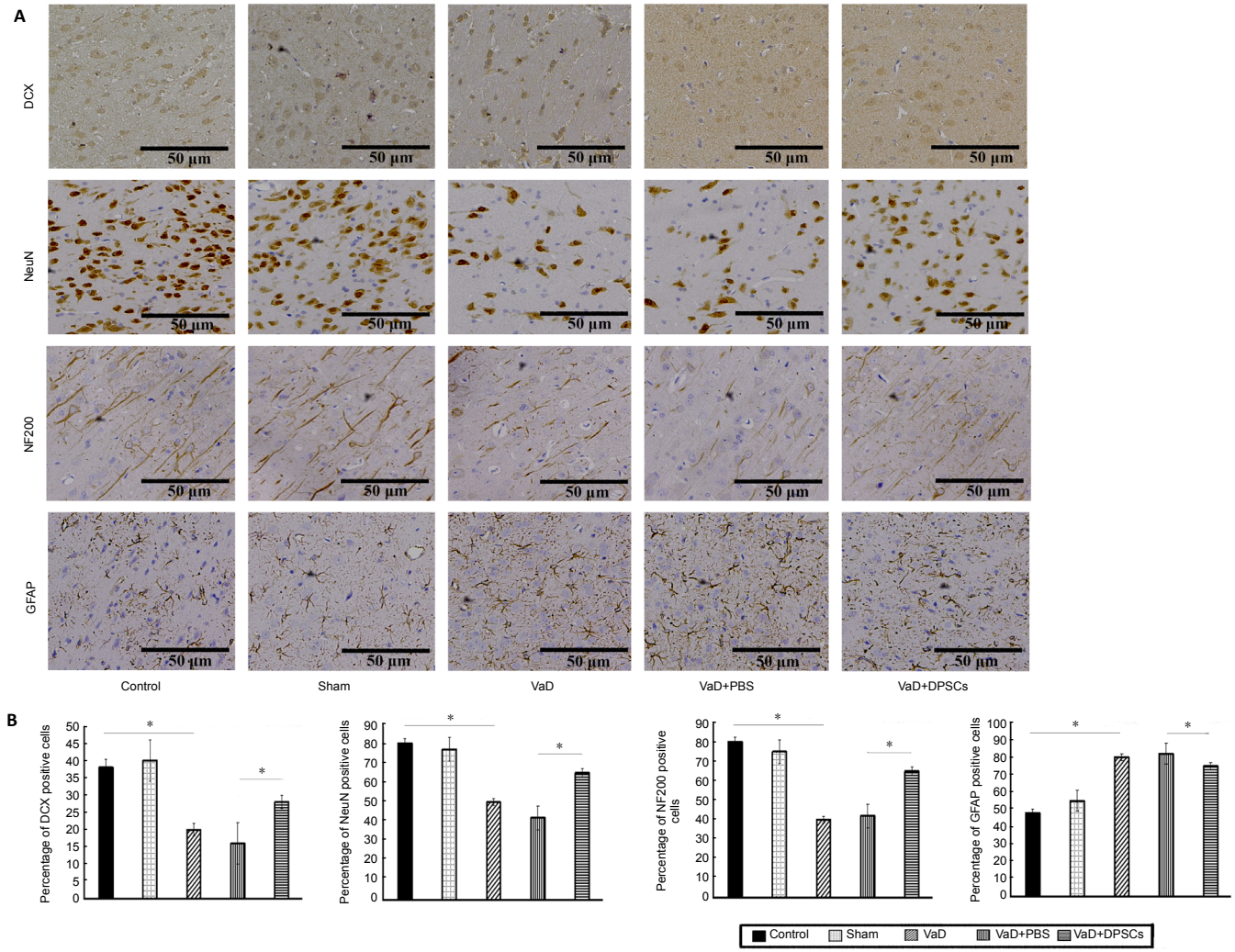

Figure 4 | **Effect of DPSCs on DCX, NF200, and NeuN positive cells in the cerebral cortex of VaD rats detected by immunohistochemical staining.**
(A) Immunohistochemical staining of DCX, NF200, NeuN, and GFAP (brown). Scale bars: 50 μm. (B) Quantitative results of the percentages of DCX, NF200, NeuN, and GFAP positive cells. The percentages of DCX, NF200, and NeuN positive cells in the VaD + DPSCs group were higher than those in the VaD + PBS group, and the percentages of DCX, NF200, and NeuN positive cells in the VaD group were lower than those in the control group. The percentage of GFAP positive cells in the VaD + DPSCs group was lower than that in the VaD + PBS group, and the percentage of GFAP positive cells in the VaD group was higher than that in the control group. Data are expressed as the mean ± SD (n = 5) and were analyzed by one-way analysis of variance. *P < 0.05. DCX: Doublecortin; DPSCs: dental pulp stem cells; GFAP: glial fibrillary acidic protein; NeuN: neuronal nuclear protein; NF200: neurofilament 200; PBS: phosphate buffered saline; VaD: vascular dementia.

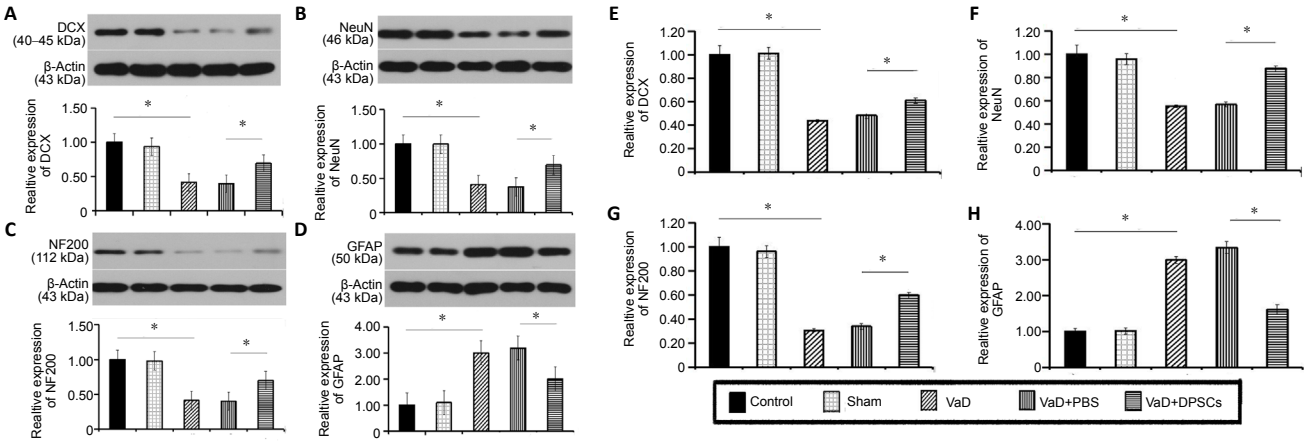

Figure 5 | **Effect of DPSCs on the mRNA and protein expression of DCX, NF200, and NeuN in the cerebral cortex of VaD rats.**
(A–D) Western blot results of the expression of DCX (A), NeuN (B), NF200 (C), and GFAP (D). (E–H) Real-time polymerase chain reaction results for the mRNA expression of DCX (E), NeuN (F), NF200 (G), and GFAP (H). The relative protein expression was expressed as the optical density ratio of target protein to β-actin in A–D. The relative mRNA expression was expressed as the optical density ratio of target mRNA to sham in E–H. Data are expressed as the mean ± SD (n = 5) and were analyzed by one-way analysis of variance. *P < 0.05. DCX: Doublecortin; DPSCs: dental pulp stem cells; GFAP: glial fibrillary acidic protein; NeuN: neuronal nuclear; NF200: neurofilament 200; PBS: phosphate buffered saline; VaD: vascular dementia.

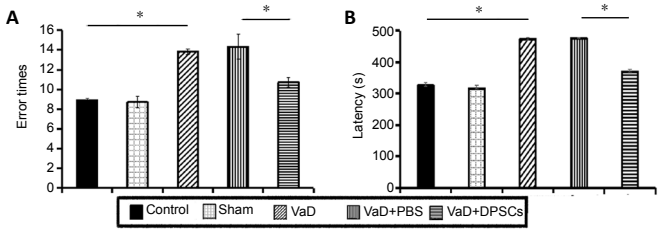

Figure 6 | **Effect of DPSCs on the neurobehavioral performance of VaD rats detected by the eight-arm maze test.**
(A) Number of errors; (B) latency. Data are expressed as the mean ± SD (n = 5) and were analyzed by one-way analysis of variance. *P < 0.05. DPSCs: Dental pulp stem cells; PBS: phosphate buffered saline; VaD: vascular dementia.

journal, and articles are distributed under the terms of the Creative Commons Attribution-NonCommercial-ShareAlike 4.0 License, which allows others to remix, tweak, and build upon the work non-commercially, as long as appropriate credit is given and the new creations are licensed under the identical terms.

Open peer reviewers: *Willian Orlando Castillo, Universidade de Sao Paulo, Brazil; Roberto Paganelli, D'Annunzio University of Chieti–Pescara, Italy.*
Additional file: *Open peer review reports 1 and 2.*

References

Baskys A, Cheng JX (2012) Pharmacological prevention and treatment of vascular dementia: approaches and perspectives. Exp Gerontol 47:887-891.
Cao XF, Jin SZ, Sun L, Zhan YB, Lin F, Li Y, Zhou YL, Wang XM, Gao L, Zhang B (2017) Therapeutic effects of hepatocyte growth factor-overexpressing dental pulp stem cells on liver cirrhosis in a rat model. Sci Rep 7:15812.
Farkas E, Luiten PG, Bari F (2007) Permanent, bilateral common carotid artery occlusion in the rat: a model for chronic cerebral hypoperfusion-related neurodegenerative diseases. Brain Res Rev 54:162-180.
Fawcett JW, Asher RA (1999) The glial scar and central nervous system repair. Brain Res Bull 49:377-391.
Gandia C, Armiñan A, García-Verdugo JM, Lledó E, Ruiz A, Miñana MD, Sanchez-Torrijos J, Payá R, Mirabet V, Carbonell-Uberos F, Llop M, Montero JA, Sepúlveda P (2008) Human dental pulp stem cells improve left ventricular function, induce angiogenesis, and reduce infarct size in rats with acute myocardial infarction. Stem Cells 26:638-645.
Gronthos S, Mankani M, Brahim J, Robey PG, Shi S (2000) Postnatal human dental pulp stem cells (DPSCs) in vitro and in vivo. Proc Natl Acad Sci U S A 97:13625-13630.
He Y, Jin X, Wang J, Meng M, Hou Z, Tian W, Li Y, Wang W, Wei Y, Wang Y, Meng H, Lu X, Chen Z, Fu L (2017) Umbilical cord-derived mesenchymal stem cell transplantation for treating elderly vascular dementia. Cell Tissue Bank 18:53-59.
Jin BR, Liu HY (2019) Comparative efficacy and safety of cognitive enhancers for treating vascular cognitive impairment: systematic review and Bayesian network meta-analysis. Neural Regen Res 14:805-816.
Huang AH, Snyder BR, Cheng PH, Chan AW (2008) Putative dental pulp-derived stem/stromal cells promote proliferation and differentiation of endogenous neural cells in the hippocampus of mice. Stem Cells 26:2654-2663.
Király M, Kádár K, Horváthy DB, Nardai P, Rácz GZ, Lacza Z, Varga G, Gerber G (2011) Integration of neuronally predifferentiated human dental pulp stem cells into rat brain in vivo. Neurochem Int 59:371-381.
Kurzina NP, Aristova IY, Volnova AB, Gainetdinov RR (2020) Deficit in working memory and abnormal behavioral tactics in dopamine transporter knockout rats during training in the 8-arm maze. Behav Brain Res 390:112642.
Liu W, Wang Y, Gong F, Rong Y, Luo Y, Tang P, Zhou Z, Zhou Z, Xu T, Jiang T, Yang S, Yin G, Chen J, Fan J, Cai W (2019) Exosomes derived from bone mesenchymal stem cells repair traumatic spinal cord injury by suppressing the activation of A1 neurotoxic reactive astrocytes. J Neurotrauma 36:469-484.
Luo Z, Wu F, Xue E, Huang L, Yan P, Pan X, Zhou Y (2019) Hypoxia preconditioning promotes bone marrow mesenchymal stem cells survival by inducing HIF-1α in injured neuronal cells derived exosomes culture system. Cell Death Dis 10:134.
Mawuenyega KG, Sigurdson W, Ovod V, Munsell L, Kasten T, Morris JC, Yarasheski KE, Bateman RJ (2010) Decreased clearance of CNS beta-amyloid in Alzheimer's disease. Science 330:1774.
Mead B, Logan A, Berry M, Leadbeater W, Scheven BA (2017) Concise review: Dental pulp stem cells: A novel cell therapy for retinal and central nervous system repair. Stem Cells 35:61-67.
Mullen RJ, Buck CR, Smith AM (1992) NeuN, a neuronal specific nuclear protein in vertebrates. Development 116:201-211.
Nagyova M, Slovinska L, Blasko J, Grulova I, Kuricova M, Cigankova V, Harvanova D, Cizkova D (2014) A comparative study of PKH67, DiI, and BrdU labeling techniques for tracing rat mesenchymal stem cells. In Vitro Cell Dev Biol Anim 50:656-663.
Nanri M, Watanabe H (1999) Availability of 2VO rats as a model for chronic cerebrovascular disease. Nihon Yakurigaku Zasshi 113:85-95.
Nicola FDC, Marques MR, Odorcyk F, Arcego DM, Petenuzzo L, Aristimunha D, Vizuete A, Sanches EF, Pereira DP, Maurmann N, Dalmaz C, Pranke P, Netto CA (2017) Neuroprotector effect of stem cells from human exfoliated deciduous teeth transplanted after traumatic spinal cord injury involves inhibition of early neuronal apoptosis. Brain Res 1663:95-105.
Porseva VV (2013) Topography and morphometric characteristics of NF200(+)-neurons of the spinal cord gray matter after deafferentation with capsaicin. Morfologiia 144:20-25.
Rockwood K, Wentzel C, Hachinski V, Hogan DB, MacKnight C, McDowell I (2000) Prevalence and outcomes of vascular cognitive impairment. Vascular Cognitive Impairment Investigators of the Canadian Study of Health and Aging. Neurology 54:447-451.
Shi Y, Hu X, Zhang X, Cheng J, Duan X, Fu X, Zhang J, Ao Y (2019) Superoxide dismutase 3 facilitates the chondrogenesis of bone marrow-derived mesenchymal stem cells. Biochem Biophys Res Commun 509:983-987.
Soria G, Tudela R, Márquez-Martín A, Camón L, Batalle D, Muñoz-Moreno E, Eixarch E, Puig J, Pedraza S, Vila E, Prats-Galino A, Planas AM (2013) The ins and outs of the BCCAo model for chronic hypoperfusion: a multimodal and longitudinal MRI approach. PLoS One 8:e74631.
Suh SW, Shin BS, Ma H, Van Hoecke M, Brennan AM, Yenari MA, Swanson RA (2008) Glucose and NADPH oxidase drive neuronal superoxide formation in stroke. Ann Neurol 64:654-663.
Venkat P, Chopp M, Chen J (2015) Models and mechanisms of vascular dementia. Exp Neurol 272:97-108.
Walker EJ, Rosenberg GA (2010) Divergent role for MMP-2 in myelin breakdown and oligodendrocyte death following transient global ischemia. J Neurosci Res 88:764-773.
Wilhelmsson U, Pozo-Rodrigalvarez A, Kalm M, de Pablo Y, Widestrand Å, Pekna M, Pekny M (2019) The role of GFAP and vimentin in learning and memory. Biol Chem 400:1147-1156.
Williams PS, Spector A, Orrell M, Rands G (2000) Aspirin for vascular dementia. Cochrane Database Syst Rev:CD001296.
Woods EJ, Perry BC, Hockema JJ, Larson L, Zhou D, Goebel WS (2009) Optimized cryopreservation method for human dental pulp-derived stem cells and their tissues of origin for banking and clinical use. Cryobiology 59:150-157.
Yalvaç ME, Yarat A, Mercan D, Rizvanov AA, Palotás A, Şahin F (2013) Characterization of the secretome of human tooth germ stem cells (hTGSCs) reveals neuro-protection by fine-tuning micro-environment. Brain Behav Immun 32:122-130.
Yamamoto H, Schmidt-Kastner R, Hamasaki DI, Yamamoto H, Parel JM (2006) Complex neurodegeneration in retina following moderate ischemia induced by bilateral common carotid artery occlusion in Wistar rats. Exp Eye Res 82:767-779.
Yang KL, Chen MF, Liao CH, Pang CY, Lin PY (2009) A simple and efficient method for generating Nurr1-positive neuronal stem cells from human wisdom teeth (tNSC) and the potential of tNSC for stroke therapy. Cytotherapy 11:606-617.
Zhang XM, Du F, Yang D, Yu CJ, Huang XN, Liu W, Fu J (2010) Transplanted bone marrow stem cells relocate to infarct penumbra and co-express endogenous proliferative and immature neuronal markers in a mouse model of ischemic cerebral stroke. BMC Neurosci 11:138.
Zhang XM, Du F, Yang D, Wang R, Yu CJ, Huang XN, Hu HY, Liu W, Fu J (2011) Granulocyte colony-stimulating factor increases the therapeutic efficacy of bone marrow mononuclear cell transplantation in cerebral ischemia in mice. BMC Neurosci 12:61.
Zhu NW, Yin XL, Lin R, Fan XL, Chen SJ, Zhu YM, Zhao XZ (2020) Possible mechanisms of lycopene amelioration of learning and memory impairment in rats with vascular dementia. Neural Regen Res 15:332-341.

P-Reviewers: Castillo WO, Paganelli R; C-Editor: Zhao M; S-Editors: Yu J, Li CH; L-Editors: Kreiner L, Yu J, Song CP; T-Editor: Jia Y